Geoscience Frontiers 10 (2019) 2007–2019

HOSTED BY

ELSEVIER

Contents lists available at ScienceDirect

China University of Geosciences (Beijing)

Geoscience Frontiers

journal homepage: www.elsevier.com/locate/gsf

Research Paper

Cordierite-bearing granulites from Ihosy, southern Madagascar: Petrology, geochronology and regional correlation of suture zones in Madagascar and India

Li Tang [a,b], Meng Pan [b], Toshiaki Tsunogae [b,c,*], Yusuke Takamura [b], Yukiyasu Tsutsumi [d], N.O.T. Rakotonandrasana [e]

[a] School of Earth Sciences and Resources, China University of Geosciences Beijing, 29 Xueyuan Road, Beijing, 100083, China
[b] Graduate School of Life and Environmental Sciences, University of Tsukuba, Ibaraki, 305-8572, Japan
[c] Department of Geology, University of Johannesburg, Auckland Park, 2006, South Africa
[d] Department of Geology and Paleontology, National Museum of Nature and Science, Ibaraki, 305-0005, Japan
[e] Yokohama National University, Yokohama, 240-8501, Japan

ARTICLE INFO

Article history:
Received 8 October 2017
Received in revised form
28 March 2018
Accepted 27 May 2018
Available online 3 July 2018

Keywords:
Pseudosection modelling
Cordierite-bearing granulite
Detrital zircon geochronology
Madagascar
Gondwana supercontinent

ABSTRACT

Madagascar, a major fragment of Gondwana, is mainly composed of Precambrian basement rocks formed by Mesoarchean to Neoproterozoic tectono-thermal events and recording a Pan-African metamorphic overprint. The Ranotsara Shear Zone in southern Madagascar has been correlated with shear zones in southern India and eastern Africa in the reconstruction of the Gondwana supercontinent. Here we present detailed petrology, mineral chemistry, metamorphic *P–T* constraints using phase equilibrium modelling and zircon U-Pb geochronological data on high-grade metamorphic rocks from Ihosy within the Ranotsara Shear Zone. Garnet-cordierite gneiss from Ihosy experienced two stages of metamorphism. The peak mineral assemblage is interpreted as garnet + sillimanite + cordierite + quartz + plagioclase + K-feldspar + magnetite + spinel + ilmenite, which is overprinted by a retrograde mineral assemblage of biotite + garnet + cordierite + quartz + plagioclase + K-feldspar + magnetite + spinel + ilmenite. Phase equilibria modelling in the system Na_2O–CaO–K_2O–FeO–MgO–Al_2O_3–SiO_2–H_2O–TiO_2–Fe_2O_3 (NCKFMASHTO) indicates peak metamorphic conditions of 850–960 °C and 6.9–7.7 kbar, and retrograde *P–T* conditions of <740 °C and <4.8 kbar, that define a clockwise *P–T* path. Near-concordant ages of detrital zircon grains in the garnet-cordierite gneiss dominantly exhibit ages between 2030 Ma and 1784 Ma, indicating dominantly Paleoproterozoic sources. The lower intercept age of 514 ± 33 Ma probably indicates the timing of high-grade metamorphism, which coincides with the assembly of the Gondwana supercontinent. The comparable rock types, zircon ages and metamorphic *P–T* paths between the Ranotsara Shear Zone and the Achankovil Suture Zone in southern India support an interpretation that the Ranotsara Shear Zone is a continuation of the Achankovil Suture Zone.

1. Introduction

The 'Pan-African' orogeny (Kennedy, 1964) is the dominant tectono-thermal event during the Neoproterozoic to Cambrian (between 950 Ma and 450 Ma) based on previous petrological, geochemical, and geochronological studies (e.g., Kröner, 1984). The orogeny is recorded in rocks in almost all Gondwana continental fragments (e.g. Africa, South America, Antarctica, India, Australia, Sri Lanka and Madagascar), mostly with intense deformation, high-grade metamorphism, and syn-to post-orogenic magmatic activities. Dominant collisional events of the orogeny took place at 600–500 Ma, which corresponds to the final assembly of the Gondwana supercontinent (Collins et al., 2007, 2014; Plavsa et al., 2012, 2015; Johnson et al., 2015; Li et al., 2017; Santosh et al., 2017; Tang et al., 2018). The latest Neoproterozoic to Cambrian tectono-metamorphic imprint has been investigated in most of these areas with the aim of reconstruction of the Gondwana

* Corresponding author. Graduate School of Life and Environmental Sciences, University of Tsukuba, Ibaraki, 305-8572, Japan.
E-mail address: tsunogae@geol.tsukuba.ac.jp (T. Tsunogae).
Peer-review under responsibility of China University of Geosciences (Beijing).

https://doi.org/10.1016/j.gsf.2018.05.014

history. Emphasis has been placed on the basement rocks in Africa (e.g., Mosley, 1993; Jacobs et al., 1997; de Wit et al., 2001), Antarctica (e.g., Shiraishi et al., 1994; Jacobs et al., 1998; Piazolo and Markl, 1999; Tsunogae et al., 2014, 2015, 2016; Takahashi et al., 2018; Takamura et al., 2018), India (e.g., Collins et al., 2007; Santosh et al., 2009; 2015; 2016; 2017; Tang et al., 2018), Sri Lanka (e.g., Schumacher et al., 1990; Hiroi et al., 1994; Kröner et al., 2003; Santosh et al., 2014; Takamura et al., 2015; He et al., 2016a, b), and Madagascar (e.g., Nicollet, 1985, 1990; Windley et al., 1994; Kröner et al., 1996; Martelat et al., 1997; Nicollet et al., 1997; Nédélec et al., 2000; de Wit et al., 2001).

Madagascar, located in the Indian Ocean offshore from Mozambique, is mainly composed of Precambrian basement rocks formed by Mesoarchean to Neoproterozoic tectono-thermal events and recording a Pan-African metamorphic overprint (e.g., Windley et al., 1994; Tucker et al., 1999, 2011; Boger et al., 2015; Fitzsimons, 2016; Endo et al., 2017; Rindraharisaona et al., 2017; Fig. 1). One of the most striking tectonic features of the Malagasy basement is the presence of large-scale shear zones, marked by intense deformation, high degree of partial melting, and high fluid flow (Pili et al., 1997). The NW–SE trending Ranotsara Shear Zone (Ackermand et al., 1989) is regarded as an intra-crustal mega strike-slip shear zone with a sinistral sense of shear that formed at the end of the Proterozoic (e.g., de Wit et al., 2001). It divides the Precambrian basement of Madagascar into two geologically different segments (Fig. 2; Windley et al., 1994), namely southern and central-northern Madagascar. In the past decades, previous studies have indicated varying *P–T* evolutions in Southern Madagascar (e.g., Nicollet, 1985, 1990; Ackermand et al., 1989, 1991; Kröner et al., 1996; Grégoire and Nédélec, 1997; Martelat et al., 1997, 2012; Markl et al., 2000; Raith et al., 2008; Rakotonandrasana et al., 2010; Jöns and Schenk, 2011; Tsunogae et al., 2013; Endo et al., 2017), ranging from 620 °C to 980 °C. Early researchers constrained *P–T* conditions using conventional geothermobarometry. However, phase equilibria modelling is the modern approach to constrain *P–T* conditions in natural rocks. Therefore, this study presents new petrological data from cordierite-bearing meta-pelitic rocks, combining conventional geothermobarometry and pseudosection modelling. In combination with zircon U-Pb geochronology, the results have important implications for understanding the evolution of high-grade metamorphic rocks in the Ranotsara Shear Zone and provide insights into the broader-scale tectono-thermal evolution of that segment of Gondwana.

2. Regional geology

Madagascar is underlain by various Precambrian metamorphic and magmatic rocks which accounts for around two-thirds of the island by area (Fig. 1). Madagascar is considered to have formed from a microcontinent (named Azania), which was situated between the Congo Craton of Africa and the Dharwar Craton of India during the mid Neoproterozoic (Collins and Pisarevsky, 2005). The orogens of the Paleo-Mozambique Ocean (between Azania and Dharwar Craton) and the Neo-Mozambique Ocean (between Azania and the Tanzania Craton) response to the collision of these continental blocks after the closure of oceanic basins at either side of Azania which make the Madagascar as a core area for the Gondwana reconstruction (Fitzsimons and Hulscher, 2005; Jöns and Schenk, 2011).

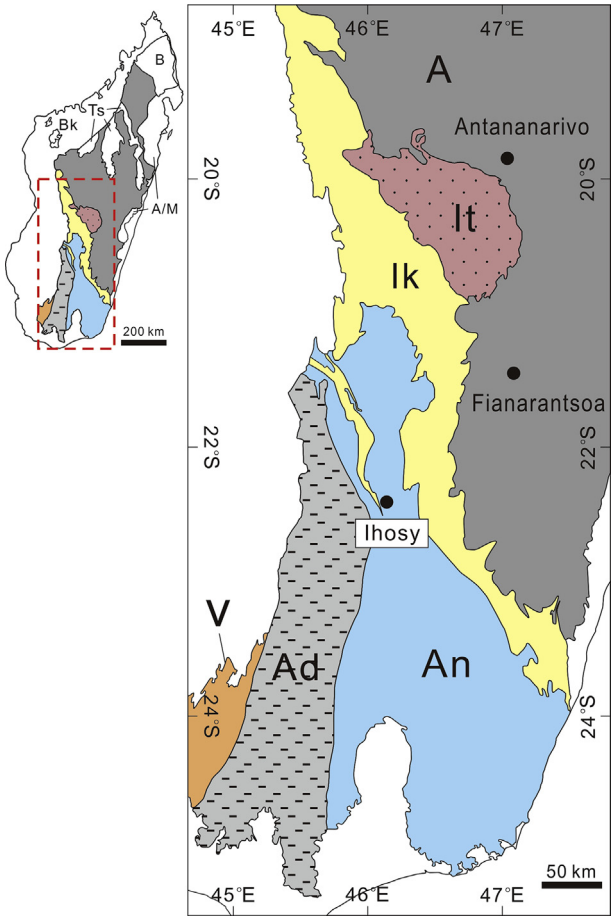

Figure 1. Map of the main tectonic units and main shear zones of Madagascar, modified after Tucker et al. (2011) and Endo et al. (2017).

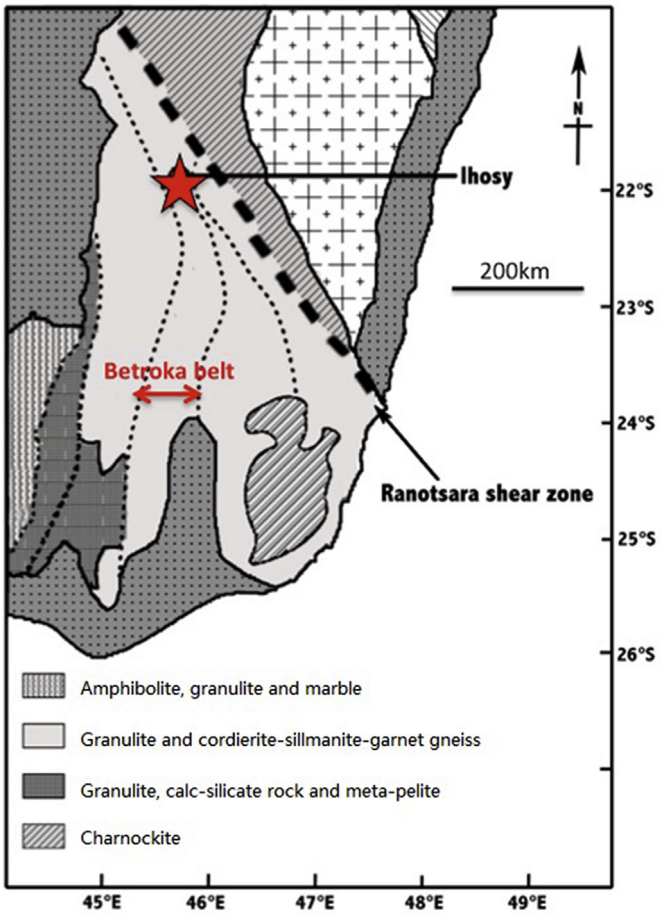

Figure 2. Simplified geological map of the southern part of Madagascar with the sample location from Ihosy (after Markl et al., 2000).

A large number of studies have used the Ranotsara Shear Zone to argue for various Gondwana reconstructions (e.g., Martelat et al., 1999; Rambeloson, 1999; Tucker et al., 1999; Chetty et al., 2003; Schreurs et al., 2006; Rakotonandrasana et al., 2010; Jöns and Schenk, 2011; Martelat et al., 2014). Previous studies have proposed that the Ranotsara Shear Zone may be correlated with various ductile shear/suture zones in southern India, such as the Achankovil Suture Zone (Drury et al., 1984; Paquette et al., 1994; Windley et al., 1994; Kriegsman, 1995; Shackleton, 1996; Windley and Razakamanana, 1996; Martelat et al., 1997; Rajesh et al., 1998; Rajesh and Chetty, 2006), the Palghat-Cauvery Suture Zone (Ackermand et al., 1991; de Wit et al., 1995; Janardhan et al., 1997; Janardhan, 1999; Harris, 1999), the Karur-Kambam-Painavu-Trichur Shear Zone (de Wit et al., 2001; Collins and Windley, 2002; Ghosh et al., 2004) and the Bhavani Shear Zone (Katz and Premoli, 1979; Agrawal et al., 1992). It also possibly correlates with the Aswa Shear Zone in Uganda and Sudan (Ackermand et al., 1991; Almond et al., 2013). Other models have argued that the Palghat-Cauvery Suture Zone is a southern continuation of the Betsimisaraka Suture at the southern margin of Neoproterozoic India (Collins and Windley, 2002; Collins et al., 2007; Strachan et al., 2007).

The Ranotsara Shear Zone divides the Precambrian Madagascar into southern and central-northern Madagascar (Fig. 2; Windley et al., 1994). Central-northern Madagascar has a prominent N–S strike and consists predominantly of granulites, gneisses and granites (Windley and Razakamanana, 1996), whereas southern Madagascar is predominantly composed of meta-igneous rocks and paragneisses that frequently contain layers and lenses of marble and quartzite. Four N–S-trending shear zones, the Ejeda, Ampanihy, Beraketa, and Tranomaro shear zones, which are up to several hundred kilometers long and several tens of kilometers wide, dissect the southern Madagascar (Fig. 2; Cox et al., 1998; Markl et al., 2000). Cordierite- and sillimanite-bearing metasediments are common in most belts of the zone south of Ranotsara. Nicollet (1985) undertook a detailed petrologic study of Precambrian migmatitic gneisses near Ihosy, and suggested migmatization at 5–5.5 kbar and >700 °C. A paragneiss in the Ranotsara Shear Zone near Ihosy yielded ages of 481 ± 41 Ma that was interpreted to represent the timing of ductile deformation and uplift during the late stages of collision tectonics (Kröner et al., 1996). Collins et al. (2012) examined samples from Ihosy and obtained a metamorphic age of 531 ± 7 Ma for zircons from the Androyen Series.

3. Sampling and petrography

3.1. Field occurrence

Representative high-grade metamorphic rock samples were collected from a large quarry of charnockite named Colline de Lalanandro located at about 2 km east of Ihosy. The quarry is composed dominantly of interlayered cordierite-biotite-sillimanite gneiss (Fig. 3a), and garnet-cordierite gneiss (Fig. 3b), which occur as layers of about 2 cm to 20 cm in thickness and 50 cm to ~2 m in length parallel to the foliation of host charnockite. Such cordierite-, sillimanite-, garnet- and biotite-rich layers are highly foliated, and dominantly alternate with cordierite-bearing leucocratic (quartzo-feldspathic) rocks (Fig. 3b and c). The leucocratic rock, which is composed of quartz, cordierite and feldspar, is massive or slightly foliated and medium to coarse grained in hand specimen. Minor amphibolite also occurs as layers or lenses distributed parallel to

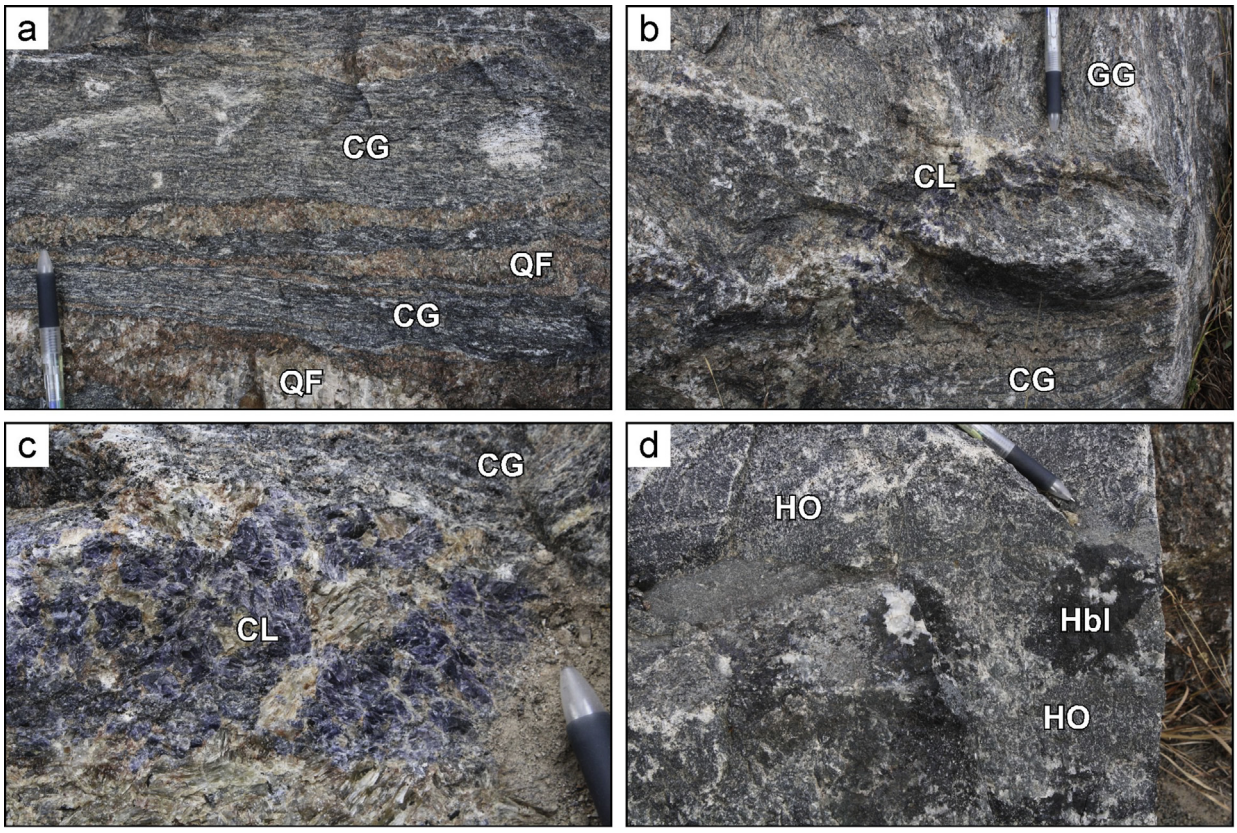

Figure 3. Field photographs of the samples discussed in this study. (a) Well-foliated and bluish Crd-Bt-Sil gneiss (CG; sample MGK2-5D) interlayered with quartzo-feldspathic rock (QF). (b) Interlayered Crd-Bt-Sil gneiss and Grt-Crd gneiss (GG; sample MGK2-5I) with a discordant vein of Crd-bearing leucocratic rock (CL). (c) Coarse-grained and bluish cordierite in the matrix of pinkish K-feldspar and quartz in Crd-bearing leucocratic rock (CL; sample MGK2-5D). (d) Coarse-grained calcic amphibole (Hbl) in amphibolite (HO) (sample MGK2-5J).

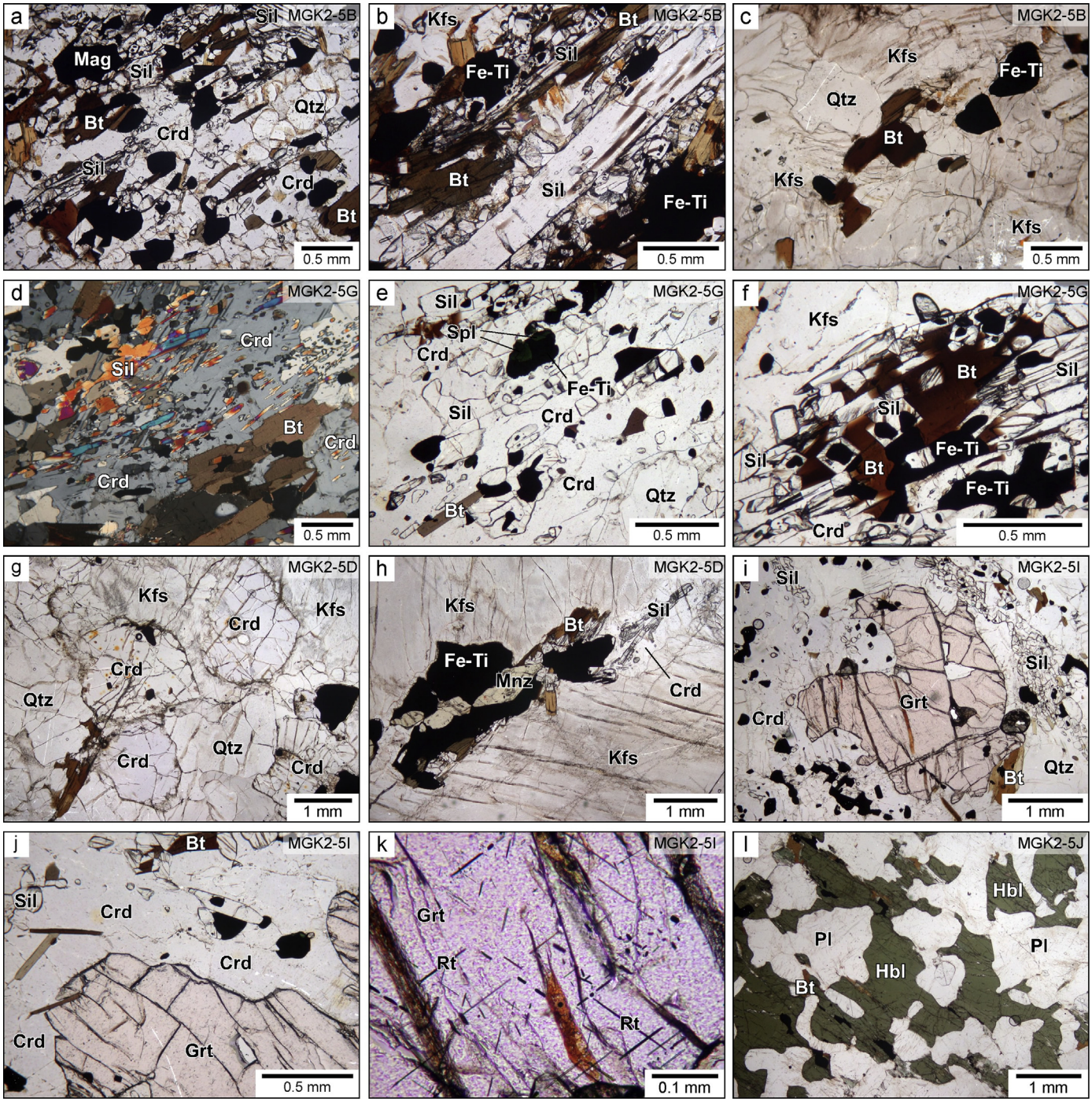

Figure 4. Representative photomicrographs of thin sections of the samples discussed in this study. (a) Abundant cordierite, biotite and sillimanite in foliated Crd-Bt-Sil gneiss (MGK2-5B). (b) Tabular sillimanite intergrowing with biotite, magnetite and ilmenite (MGK2-5B). (c) Quartzo-feldspathic layer of the Crd-Bt-Sil gneiss with abundant K-feldspar and quartz (MGK2-5B). (d) Poikiloblastic cordierite with abundant inclusions of sillimanite in Crd-Bt-Sil gneiss (MGK2-5G). (e) Sillimanite + biotite + Fe-Ti oxide intergrowth in the matrix of cordierite (MGK2-5G). (f) Subidioblastic biotite in the matrix of sillimanite and Fe-Ti oxide (MGK2-5G). (g) Large subidioblastic cordierite and K-feldspar in Crd-bearing leucocratic rock (MGK2-5D). (h) Aggregates of biotite, sillimanite, monazite and Fe-Ti oxide distributed along the grain boundary of coarse-grained K-feldspar (MGK2-5D). (i) Porphyroblastic garnet in the matrix of fine-grained sillimanite, biotite, quartz, Fe-Ti oxide and cordierite in Grt-Crd gneiss (MGK2-5I). (j) Cordierite corona around garnet probably formed by a retrograde reaction Grt + Sil + Qtz => Crd (MGK2-5I). (k) Rutile needles in garnet suggesting exsolution during post-peak cooling (MGK2-5I). (l) Coarse-grained calcic amphibole + plagioclase association in amphibolite (MGK2-5J). Mineral name abbreviations are after Kretz (1983). Fe-Ti: Fe-Ti oxide (magnetite-ilmenite intergrowth). Mineral abbreviations: Mag, Magnetite; Sil, sillimanite; Qtz, quartz; Bt, biotite; Crd, cordierite; Kfs, K-feldspar; Mnz, Monazite; Grt, garnet; Rt, Rutile; Pl, plagioclase; Hbl, hornblende.

the foliation (Fig. 3d). Such cordierite gneiss-charnockite-amphibolite associations are commonly observed in the Achankovil Suture Zone in southern India (e.g., Santosh, 1987; Ishii et al., 2006; Shimizu and Tsunogae, 2010).

3.2. Petrography

Below we briefly describe the salient petrological features of representative rocks including cordierite-biotite-sillimanite gneiss (MGK2-5B and MGK2-5G), cordierite-bearing leucocratic rock

Table 1
Mineral assemblages of rock samples investigated in this study. Mineral name abbreviations are after Kretz (1983).

Sample	Rock type	Crd	Bt	Sil	Qtz	Kfs	Pl	Grt	Mt (Spl)	Ilm	Crn	Hbl
MGK2-5B	Crd-Bt-Sil gneiss	+++	++	+	+	+	+	-	+	+	+	-
MGK2-5D	Crd-bearing leucocratic rock	+++	+	+	-	++	++	-	+	+	-	-
MGK2-5G	Crd-Bt-Sil gneiss	++	+	++	++	++	++	-	+	+	-	-
MGK2-5I	Grt-Crd gneiss	++	++	+	+	++	+	+++	+	+	-	-
MGK2-5J	Amphibolite	-	+	-	++	-	+++	-	+	-	-	+++

Mineral abbreviations: Grt, garnet; Crd, cordierite; Qtz, quartz; Pl, plagioclase; Bt, biotite; Mt, magnetite; Ilm, ilmenite; Spl, spinel; Kfs, K-feldspar; Sil, sillimanite; Crn, corundum; Hbl, hornblende.
+++: abundant, ++: moderate, +: rare, -: absent.

(MGK2-5D), garnet-cordierite gneiss (MGK2-5I), and amphibolite (MGK2-5J) from the quarry. The textural features are shown in Fig. 4. Mineral assemblages and approximate modal abundances of minerals are listed in Table 1.

3.2.1. Cordierite-biotite-sillimanite gneiss

Cordierite-biotite-sillimanite (Crd-Bt-Sil) gneiss is the dominant rock type in the Ihosy quarry (samples MGK2-5B and MGK2-5G). In hand specimen, the rocks show weak migmatization with patches composed of feldspars, quartz and cordierite, and the foliation is defined by aligned biotite flakes and sillimanite needles (Fig. 3a).

Sample MGK2-5B is composed mainly of cordierite (20%–30%), biotite (10%–15%), sillimanite (15%–25%), K-feldspar (5%–10%), plagioclase (5%–10%) and quartz (15%–25%) with minor spinel, corundum and magnetite (Fig. 4a). Cordierite (0.2–1 mm) occurs as porphyroblastic crystals in a quartzo-feldspathic matrix, and includes biotite, sillimanite, K-feldspar, plagioclase and quartz (0.03–0.5 mm) (Fig. 4a). Sillimanite (0.02–0.3 mm) occurs as tabular crystals within cordierite or forms intergrowths with biotite and quartz (Fig. 4b), possibly suggesting the progress of the following retrograde hydration reaction: Crd + Kfs ± Grt + H_2O => Bt + Sil + Qtz (Bucher and Frey, 1994). Sub-idioblastic biotite (0.01–0.2 mm) has a distinctively reddish brown color and coexists with feldspars (0.03–0.5 mm), quartz (0.02–0.5 mm) and sillimanite, and, in some cases, with cordierite. Biotite also occurs around the margins of magnetite, corundum and sillimanite. The quartzo-feldspathic layer of the sample (Fig. 3a) is composed of K-feldspar (70%–80%), quartz (20%–50%), biotite (5%–10%), minor plagioclase and Fe-Ti oxide (Fig. 4c).

Sample MGK2-5G comprises cordierite (20%–30%), sillimanite (15%–20%), biotite (10%–15%), K-feldspar (10%–15%), plagioclase (10%–15%) and quartz (5%–7%) as well as accessory magnetite and ilmenite. Cordierite (0.05–5 mm) forms large poikiloblasts as well as xenoblastic matrix grains (Fig. 4d). Sillimanite (0.1–3 mm) occurs as large fibroblastic aggregates in the matrix and as intergrowths with Fe-Ti oxide (magnetite + ilmenite + green spinel) (Fig. 4e). Magnetite and spinel show a close spatial association (Fig. 4e), interpreted as a product of exsolution during cooling (e.g., Ishii et al., 2006). Biotite (0.01–0.8 mm) also occurs in the quartzo-feldspathic matrix. In some places, biotite is present in the matrix along with sillimanite and Fe-Ti oxide (magnetite-ilmenite intergrowth) (Fig. 4f).

3.2.2. Cordierite-bearing leucocratic rock

Sample MGK2-5D contains cordierite (25%–35%), K-feldspar (35%–45%), plagioclase (5%–15%), biotite (5%–10%) and sillimanite (5%–10%) with accessory spinel, monazite, sillimanite, magnetite and ilmenite. The finely banded migmatitic texture within the Crd-Bt-Sil and Grt-Crd gneisses is consistent with in-situ partial melting. In general, cordierite (0.1–5 mm) and K-feldspar (0.1–5 mm) form large subidioblastic grains (Fig. 4g). Sillimanite (0.01–0.09 mm) occurs as fibrolite or prismatic crystals along the margins of porphyroblastic minerals (Fig. 4h) or included within cordierite porphyroblasts. Xenoblastic biotite (0.01–0.05 mm) is present at the margins of feldspar, spinel, magnetite and ilmenite (Fig. 4h).

3.2.3. Garnet-cordierite gneiss

The garnet-cordierite (Grt-Crd) gneiss is a coarse-grained granulite-facies rock with a probable pelitic protolith. The mineralogy of representative sample MGK2-5I is composed of garnet (10%–20%), cordierite (15%–20%), K-feldspar (15%–20%), biotite (10%–15%), plagioclase (15%–20%), quartz (10%–20%) and sillimanite (5–10%) with accessory spinel, magnetite and ilmenite. Garnet is coarse grained (~8 mm), poikiloblastic, and contains numerous fine-grained inclusions of biotite, sillimanite and quartz (0.02–0.2 mm) (Fig. 4i). Cordierite (0.2–5 mm) is also poikiloblastic and contains sillimanite, biotite and Fe-Ti oxide, whereas it also occurs as coronae around porphyroblastic garnet in melanocratic layers (Fig. 4j) or as rare inclusions in garnet. Rutile needles are present in the porphyroblastic garnet (Fig. 4k). Sillimanite (0.01–0.2 mm) occurs in the matrix and is aligned along the foliation defined by biotite flakes. Biotite (0.01–0.4 mm) occurs as medium-grained (1–2 mm) laths dominantly with garnet and cordierite, and is rare in the matrix. In the leucocratic layers, xenoblastic K-feldspar is medium to coarse grained (0.4–1.2 mm) and is interstitial to plagioclase and quartz.

The corona texture of cordierite suggests the progress of the following retrograde reaction: Grt + Sil + Qtz => Crd, which has been regarded as a common decompression reaction in many pelitic granulites worldwide (e.g., Harley, 1989). The retrograde metamorphism is also defined by the exsolution of rutile needles during post-peak cooling and the occurrence of spinel + ilmenite + magnetite association which is interpreted as a retrograde feature (e.g., Ishii et al., 2006).

3.2.4. Amphibolite

The amphibolite (sample MGK2-5J; Fig. 3d) comprises calcic amphibole (30%–40%), plagioclase (30%–40%), quartz (10%–20%) and biotite (<5%), with minor calcite, magnetite and ilmenite (Fig. 4l). Plagioclase is subidioblastic to xenoblastic, coarse grained (0.3–3 mm), and often shows a granoblastic texture. Calcic amphibole is greenish-brown in color, coarse grained (0.5–4 mm), xenoblastic, and partly surrounded by brownish biotite (0.1–0.4 mm). Rare quartz (0.02–0.1 mm) occurs at the margins of plagioclase and calcic amphibole.

4. Analytical techniques

4.1. Mineral chemistry

Mineral chemical analyses were carried out using an electron microprobe analyzer (JEOL JXA8530F) at the Chemical Analysis Division of the Research Facility Center for Science and Technology, the University of Tsukuba. The analyses were performed using a 15 kV accelerating voltage and 10 nA sample current, and the data were regressed using an oxide-ZAF correction program supplied by JEOL. The detection limits are 0.01 wt.%.

4.2. Whole-rock geochemistry

Whole rock major elements were analyzed at the Activation Laboratories, Ontario, Canada. Fresh rock chips were initially reduced to avoid surface weathering. Contents of major elemental oxides were measured by 'lithium metaborate/tetraborate fusion ICP whole rock (Code 4B)', and the fused samples were diluted and analyzed by Perkin Elmer Sciex ELAN 6000, 6100 or 9000 ICP/MS. The detection limits of major elements are 0.01 wt.%. The detailed analytical conditions and detection limits are summarized at http://www.actlabs.com/.

4.3. Zircon geochronology

A fresh Grt-Crd gneiss sample (MGK2-5I) was crushed and milled, followed by gravimetric and magnetic separation and hand picking of zircon grains under a binocular microscope. Representative zircon grains, zircon standard FC1 ($^{206}Pb/^{238}U$ = 0.1859; Paces and Miller, 1993) and NIST SRM 610 standard glass were mounted on a transparent epoxy resin disk and then polished to expose the crystals. Backscattered electron and cathodoluminescence (CL) images, and U–Th–Pb isotopic analyses were performed at National Museum of Nature and Science, Japan. Zircon U–Pb analyses were conducted using an Agilent 7700x inductively coupled plasma mass spectrometer (ICP-MS) equipped with ESI NWR213 laser ablation system. Detailed analytical procedures and work conditions are described in Tsutsumi et al. (2012). A Nd-YAG laser (213 nm wavelength and 5 ns pulse), with a 25 μm spot size and 4–5 J/cm^2 energy were used in this study. All measurements were carried out using time resolved analysis. U and Th concentrations were calibrated by using ^{29}Si as an internal calibrant. The zircon OT4 (191 Ma, Horie et al., 2013) and NIST SRM 610 standard glass were used as the reference material. Common Pb corrections for the concordia diagrams and each age were made using ^{208}Pb on the basis of the model for common Pb compositions proposed by Stacey and Kramers (1975). Age data and plots were processed by using the Isoplot/Ex software (Ludwig, 2003).

5. Mineral chemistry

5.1. Garnet

Porphyroblastic garnet in the Grt-Crd gneiss is dominantly a solid solution between almandine and pyrope (X_{Mg} = Mg/(Fe + Mg) = 0.25–0.28) with low contents of the grossular (<3 mol.%) and spessartine (<2 mol.%) components, in which compositions change slightly from core to rim (Supplementary Table 1). In sample MGK2-5I, the garnet core shows slightly lower almandine and higher pyrope ($Alm_{69–70}Pyr_{26–27}Grs_2Sps_{2–3}$) than the rim ($Alm_{71–72}Pyr_{23–24}Grs_2Sps_{2–3}$), suggesting local Fe-Mg exchange between the garnet rim and matrix ferromagnesian minerals during retrograde metamorphism.

5.2. Biotite

Biotite is generally Mg-rich and characterized by high TiO_2 contents (up to 5.4 wt.%). Biotite inclusions (Bt-1) within garnet are relatively Mg-rich (X_{Mg} = 0.61) compared to matrix biotite (Bt-2) (X_{Mg} = 0.43–0.55), although their TiO_2 contents are almost consistent (4.2–5.4 wt.%, e.g. sample MGK2-5I; Grt-Crd gneiss). The lower X_{Mg} (0.43) is recorded in xenoblastic biotite associated with cordierite, quartz and feldspar in sample MGK2-5G (Crd-Bt-Sil gneiss), which contains intermediate TiO_2 contents of 4.8–4.9 wt.%. In contrast, biotite (Bt-3) around Fe-Ti oxides or at the margins of feldspar and sillimanite in sample MGK2-5B (Crd-Bt-Sil gneiss) shows the highest X_{Mg} (0.63–0.64) and the lowest TiO_2 contents (1.6–1.7 wt.%) consistent with a retrograde origin.

5.3. Feldspars

Plagioclase is principally albite-rich with minor orthoclase content (<2 mol.%). Plagioclase (Pl-1) in samples MGK2-5B (Crd-Bt-Sil gneiss) and MGK2-5D (Crd-bearing leucocratic rock) has a similar compositional range of $An_{33–35}Ab_{65–67}Or_{0–1}$, although mineral assemblages of the samples are slightly different. Slightly higher albite contents of $An_{9–10}Ab_{87–89}Or_{1–4}$ (Pl-2) characterise matrix plagioclase in sample MGK2-5G (Crd-Bt-Sil gneiss). Plagioclase coexisting with calcic amphibole in the amphibolite (sample MGK2-5J) (Pl-3) shows the highest anorthite content of $An_{84–86}Ab_{13–14}Or_{0–2}$ (Supplementary Table 1).

All K-feldspar grains in the Crd-Bt-Sil gneiss (samples MGK2-5B and MGK2-5G), the Grt-Crd gneiss (sample MGK2-5I) and the Crd-bearing leucocratic rock (sample MGK2-5D) show consistent orthoclase-rich compositions of $An_{0–1}Ab_{17–20}Or_{79–82}$.

5.4. Cordierite

Cordierite shows a uniform composition in all samples with X_{Mg} in the range of 0.71–0.77 (Supplementary Table 1). Cordierite (Crd-2) in the Crd-Bt-Sil gneiss (samples MGK2-5B and MGK2-5G) has consistent X_{Mg} values of 0.73–0.74. A similar X_{Mg} range (0.71–0.72) was also obtained from cordierite (Crd-2) in sample MGK2-5D (Crd-bearing leucocratic rock). Cordierite coronae (Crd-3) around porphyroblastic garnet in sample MGK2-5I (Grt-Crd gneiss) have similar X_{Mg} of 0.71, while cordierite inclusions (Crd-1) in garnet in the same sample show the highest X_{Mg} of 0.77.

5.5. Sillimanite

Fibrolitic or prismatic sillimanite (Sil-1) within porphyroblastic garnet (sample MGK2-5I; Grt-Crd gneiss) and cordierite (sample MGK2-5D; Crd-bearing leucocratic rock) contains minor Fe_2O_3 contents of 0.93–1.29 wt.%. Large prismatic sillimanite in samples MGK2-5G (Crd-Bt-Sil gneiss) and MGK2-5I (Grt-Crd gneiss) (Sil-1) shows similar Fe_2O_3 contents of 1.02–1.23 wt.%. In contrast, that in sample MGK2-5B (Crd-Bt-Sil gneiss) associated with magnetite (Sil-3) displays the highest Fe_2O_3 content of 3.34 wt.%.

5.6. Other minerals

Spinel in the studied rocks, which occurs as a retrograde mineral coexisting with cordierite, feldspar, magnetite and ilmenite, is principally a solid solution of Mg-spinel and hercynite (Fe^{2+} = 0.75–0.92 p.f.u., X_{Mg} = 0.14–0.20). It contains a small amount of Cr_2O_3 (0.28–0.39 wt.%) and ZnO (0.43–2.80 wt.%). Matrix spinel (Spl-1) coexisting with Fe-Ti oxide in sample MGK2-5B (Crd-Bt-Sil gneiss) has the highest ZnO of 2.4–2.8 wt.%. In contrast, spinel (Spl-2) within cordierite in sample MGK2-5D (Crd-bearing leucocratic rock) shows lower ZnO contents of 0.43–0.56 wt.% and a lower X_{Mg} of 0.14 (Supplementary Table 1).

The composition of ilmenite is close to its ideal formulae as $FeTiO_3$. Magnetite is also close to Fe_3O_4, with low TiO_2 (<0.06 wt.% for MGK2-5B and <0.04 wt.% for MGK2-5B). Greenish-brown xenoblastic calcic amphibole in the amphibolite (sample MGK2-5J) has X_{Mg} = 0.51–0.52 and TiO_2 = 1.60–1.77 wt.%, and is classified as pargasite (Si = 6.26–6.29 p.f.u., Al = 2.09–2.17 p.f.u., Na + K = 0.78–0.81 p.f.u.) according to the classification of Leake et al. (1997). Compositional zoning is absent in amphibole.

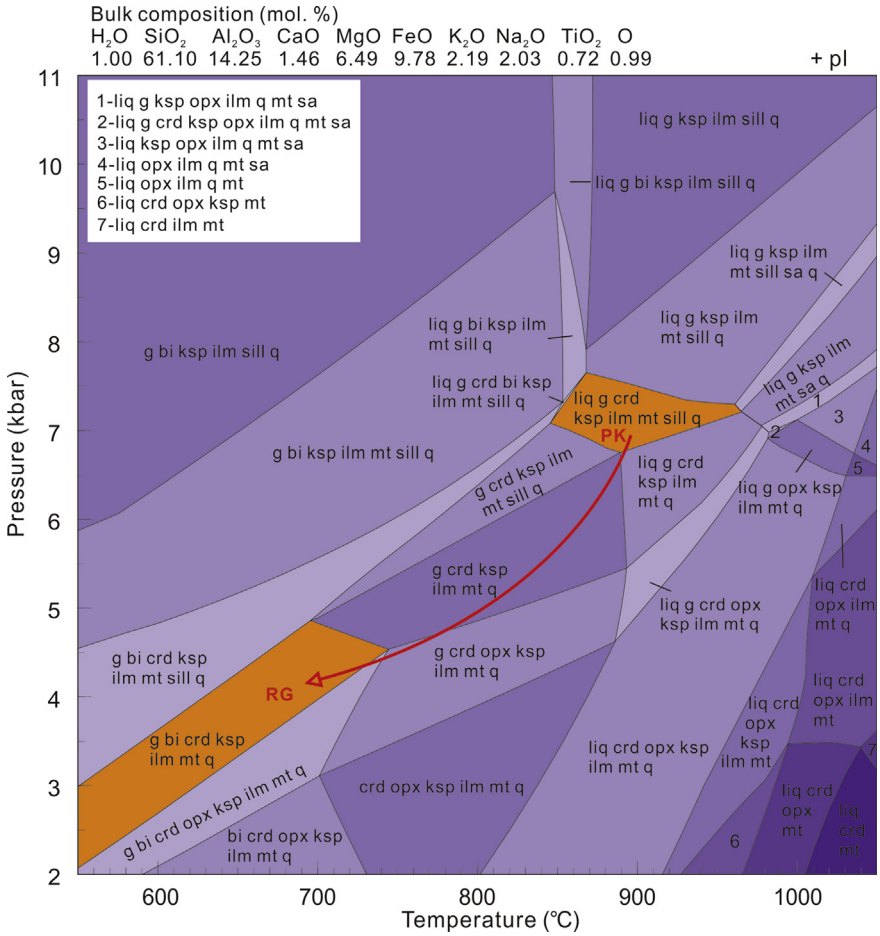

Figure 5. *P–T* pseudosection for garnet-cordierite gneiss sample MGK2-5I calculated in the system NCKFMASHTO. Mineral abbreviations: crd: cordierite, g: garnet, bi: biotite, q: quartz, ksp: K-feldspar, pl: plagioclase, sill: sillimanite, ilm: ilmenite, mt: magnetite, opx: orthopyroxene, sa: sapphirine, liq: liquid. PK: peak stage, RG: retrograde stage.

6. Phase equilibria modelling

A *P–T* pseudosection of the Grt-Crd gneiss from Ihosy, southern Madagascar, was constructed in the Na_2O–CaO–K_2O–FeO–MgO–Al_2O_3–SiO_2–H_2O–TiO_2–Fe_2O_3 (NCKFMASHTO) system (Fig. 5). For the pseudosection calculation, the effective bulk-rock composition normalized into mole proportion in the model system for sample MGK2-5I, were calculated on the basis of the bulk-rock geochemical results. MnO and Cr_2O_3 were neglected because of their low concentrations.

The *P–T* pseudosection calculations were performed using THERMOCALC 3.33 (Holland and Powell, 1998; updated October 2009) and the internally consistent thermodynamic dataset of tcds55s (Holland and Powell, 1998). The phases considered in the modelling and the corresponding activity-composition (a–x) models include garnet, biotite and melt (White et al., 2007), orthopyroxene and magnetite (White et al., 2002), plagioclase and K-feldspar (Holland and Powell, 2003), ilmenite (White et al., 2000) and cordierite (Holland and Powell, 1998). The aluminosilicates and quartz were considered as pure end-member phase. The *P–T* pseudosection was constructed in the range of 2–11 kbar and 550–1050 °C.

The *P–T* pseudosection of sample MGK2-5I (Grt-Crd gneiss) is shown in Fig. 5. In the *P–T* diagram, plagioclase is ubiquitous. Melt is predicted to be stable at high temperature (>850 °C) at which no biotite is predicted. Orthopyroxene is stable in the low pressure field and sapphirine is stable in the high *P–T* field (Fig. 5). The inferred peak mineral assemblage of garnet + cordierite (Crd-1) + sillimanite + quartz + plagioclase + K-feldspar + magnetite + ilmenite occupies a field in the range of 850–960 °C and 6.9–7.7 kbar. The peak field is confined by the cordierite-out line for the upper-pressure limit, sillimanite-out line for the lower-pressure limit, biotite-in line for the lower-temperature limit and sapphirine-in line for the upper-temperature limit. The retrograde mineral assemblage of biotite + garnet + cordierite (Crd-3) + quartz + plagioclase + K-feldspar + magnetite/spinel + ilmenite defines the *P–T* condition of <740 °C and <4.8 kbar. The retrograde field is well constrained by the sillimanite-in line that provides an upper-pressure limit, the orthopyroxene-in line as a lower-pressure limit and the biotite-out line as an upper-temperature limit. The results are consistent with a clockwise *P–T* path with a post-peak cooling and decompression process.

7. Zircon U-Pb geochronology

The results of zircon U–Pb analyses of sample MGK2-5I (Grt-Crd gneiss) is given in Supplementary Table 2. A total of sixty-one spots were analyzed from sixty zircon grains with twenty-eight grains showing <15% discordance. CL images of representative zircons are shown in Fig. 6 together with the location of analytical spots and ages. The age data are plotted in a Concordia diagram (Fig. 7a) and a histogram with probability density plot (Fig. 7b). The zircon grains have rounded to subhedral morphologies, with aspect ratios of 2:1 to 1:1, and grain sizes range from 30 μm to 150 μm. They have poorly luminescent cores surrounded by distinct bright

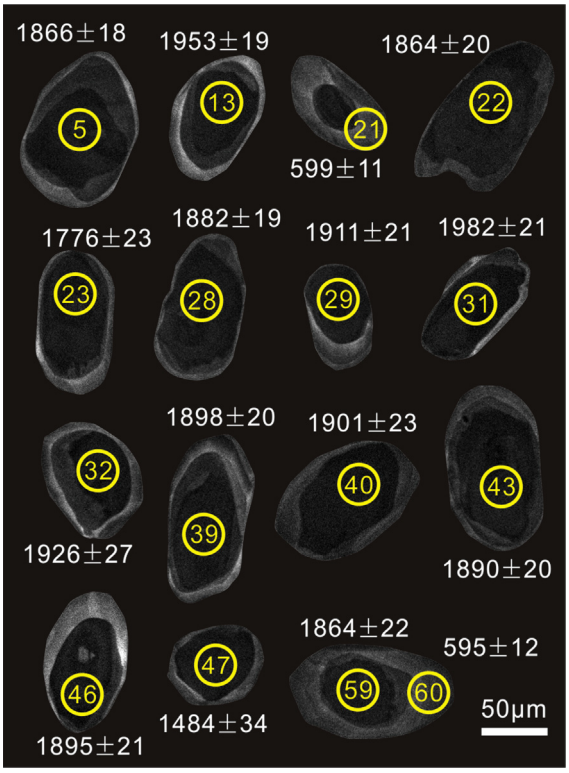

Figure 6. Cathodoluminescence (CL) images of representative zircons in garnet-cordierite gneiss sample MGK2-5I, showing analytical positions and zircon U-Pb ages (in Ma).

luminescent and thin rims. Most zircons are characterized by oscillatory-zoned or fractured heterogeneous cores with or without homogeneous mantles which separate the cores and rims. Fifty-nine ages obtained from zircon cores show $^{207}Pb/^{206}Pb$ ages ranging from 2030 ± 20 Ma to 1484 ± 34 Ma. The dominant age populations are clustered between 1953 Ma and 1769 Ma, with the second age population between 2030 Ma and 1982 Ma (Fig. 7b), whereas near-concordant data range from 2030 ± 20 Ma to 1784 ± 23 Ma. The majority of the analyzed spots are distributed along a discordia line and yields an lower intercept age of 514 ± 33 Ma, probably representing the timing of high-grade metamorphism.

8. Discussion

8.1. Metamorphic condition and evolution

Based on our petrographic and mineral compositional studies as well as the application of quantitative *P–T* pseudosection modelling using a NCKFMASHTO system, we obtained peak metamorphic conditions of 850–960 °C and 6.9–7.7 kbar which were constrained by the peak mineral assemblage of garnet + sillimanite + cordierite + K-feldspar + quartz + plagioclase + magnetite + ilmenite in sample MGK2-5I (Grt-Crd gneiss) from the studies area (Fig. 5). The stability field of the assemblage shown in Fig. 5 is located slightly above the inferred solidus of the sample, which is consistent with the limited quantity of inferred melt phases in the sample, and also common features of high-grade metamorphic rocks (Korhonen et al., 2013; Tang et al., 2017). The retrograde metamorphic *P–T* conditions are constrained by the biotite + garnet + cordierite + quartz + plagioclase + K-feldspar + magnetite/spinel + ilmenite assemblage in the same sample as <740 °C and <4.8 kbar in the pseudosection (Fig. 5). A decompressional cooling path from the peak (850–960 °C and 6.9–7.7 kbar) to a retrograde stage (<740 °C and <4.8 kbar) has been constructed in this study. The occurrence of cordierite coronae around garnet in sample MGK2-5I (Fig. 4j), which has been reported from many granulite terranes as an evidence of near-isothermal decompression, suggests that the cooling path is probably a part of clockwise *P–T* loop.

High-grade metasedimentary rocks are exposed along several localities in Ihosy from southern Madagascar and have been the focus of several studies (Nicollet, 1985, 1990; Ackermand et al., 1989; Kröner et al., 1996; Grégoire and Nédélec, 1997; Markl et al., 2000; Rakotonandrasana et al., 2010; Jöns and Schenk, 2011; Boger et al., 2012). Based on various geothermobarometric studies using various techniques, the peak pressure condition in Ihosy has been inferred to be 8-11 kbar (Markl et al., 2000), whereas temperature estimates range from 620 °C to 980 °C (e.g. Ackermand et al., 1989; Grégoire and Nédélec, 1997).

Nicollet (1985) applied garnet-cordierite and garnet-biotite geothermobarometers and obtained temperatures of more than 700 °C and pressures of 5.0–5.5 kbar. Nicollet (1990) proposed low-pressure granulite-facies condition of 650–800 °C and 4–6 kbar from Ihosy. Kröner et al. (1996) reported higher-temperature condition of 880–1060°C and 4.4–6.5 kbar. Markl et al. (2000) suggested that the region experienced an earlier high-pressure and

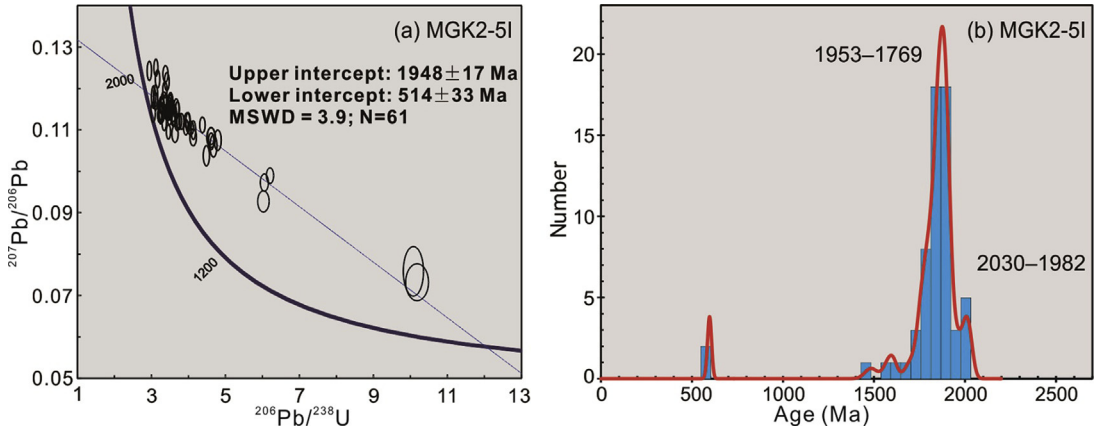

Figure 7. (a) Tera-Wasserburg concordia diagram and (b) relative probability diagram of garnet-cordierite gneiss sample MGK2-5I from Ihosy.

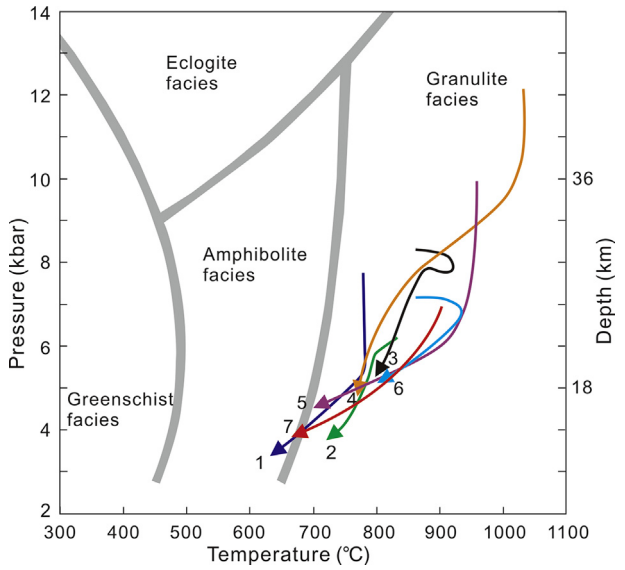

Figure 8. The comparison of *P–T* paths based on geothermobarometers and *P–T* pseudosection modelling evaluated to constrain the *P–T* evolution of the representative cordierite gneisses from the Ranotsara Shear Zone and the Achankovil Suture Zone. 1: Santosh, 1987; 2: Nandakumar and Harley, 2000; 3: Cenki et al., 2002; 4: Ishii et al., 2006; 5: Shimizu et al., 2009; 6: Johnson et al., 2015; 7: this study.

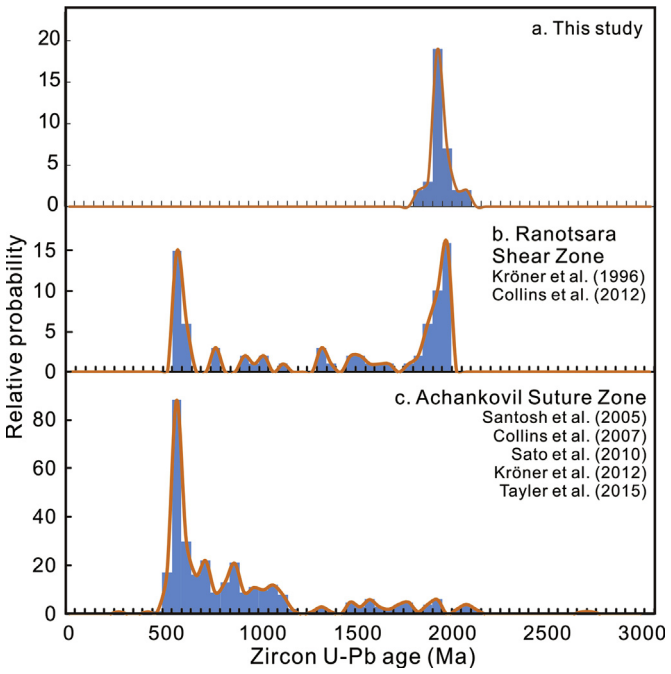

Figure 9. Summary of geochronological data for this study with discordance lower than 15% (a), the Ranotsara Shear Zone near Ihosy (b: Kröner et al., 1996; Collins et al., 2012) and the Achankovil Suture Zone (c: Santosh et al., 2005; Collins et al.,2007; Sato et al., 2010; Kröner et al., 2012; Taylor et al., 2015).

high-temperature event of ~8 kbar and ~880 °C, which was overprinted by lower-pressure metamorphism (~4 kbar). Rakotonandrasana et al. (2010) obtained the peak metamorphic conditions of the spinel-garnet-cordierite-sillimanite-bearing meta-pelites from the Betroka belt as 880–1060 °C and 4.5–6.6 kbar with a clockwise *P–T* trajectory by using WinTWQ program. Jöns and Schenk (2011) examined the petrology of meta-pelitic rock samples from the south of the Ranotsara Shear Zone near Ihosy, with ultrahigh-temperature (UHT) metamorphic *P–T* conditions in the range of 950–1000 °C and 8–11 kbar. Recently, Boger et al. (2012) interpreted the *P–T* conditions of high-grade aluminous meta-pelites from Ihosy area in the range of ~880–920°C and 6–6.5 kbar. Tsunogae et al. (2013) examined charnockite from Ihosy area and obtained high-temperature metamorphic assemblages with peak metamorphic *P–T* conditions in the range of 8–10.5 kbar and 820–880°C. Endo et al. (2017) evaluated the petrogenesis of incipient charnockite from Ambodin Ifandana area, about 48 km north of Ihosy, and estimated the condition of charnockite formation at 8.5–10.5 kbar and 880–900 °C. The results of this study on the garnet-cordierite gneiss sample of the Ihosy area in southern Madagascar confirms the high-grade metamorphism (850–960 °C and 6.9–7.7 kbar) in Ihosy area (Fig. 8).

8.2. Provenance, age constraints of deposition and metamorphism

The near-concordant (discordance <15%) detrital zircon grains in sample MGK2-5I (Grt-Crd gneiss) dominantly exhibit a wide age variation from 2030 Ma to 1784 Ma, indicating the protolith sediments were mainly sourced from Paleoproterozoic rocks (Fig. 9a). The age range is nearly consistent with that reported in previous studies (Kröner et al., 1996; Collins et al., 2012) (Fig. 9b). The style and exact timing of the Pan-African metamorphic event of Ihosy have been reported by several studies (Kröner et al., 1996, 1999; de Wit et al., 2001; Collins et al., 2012). Firstly, Kröner et al. (1996) focused on detrital zircons in metapelitic rock and sillimanite-cordierite-garnet gneiss samples from the Ihosy area that yielded ages between ~720 Ma and ~1855 Ma, suggesting a geochronologically heterogeneous source region and a depositional age of less than ~720 Ma. Moreover, Neoproterozoic zircons have also been retrieved from metasedimentary gneisses (Kröner et al., 1999; de Wit et al., 2001), demonstrating that at least some of the sedimentary protoliths were deposited in Neoproterozoic or younger times. The deposition of the Graphite and Androyen groups protoliths is poorly constrained between the late Paleoproterozoic and Cambrian (~1830–530 Ma). The protoliths of the Androyen and Graphite groups were sourced from Paleoproterozoic rocks ranging in age between 2300 Ma and 1800 Ma (Collins et al., 2012). The results of this study on the sample of the Ihosy area from the Androyen group show considerable detritus sourced from Paleoproterozoic protolith, and the depositional age is suggested as between 1784 Ma and 514 Ma based on the youngest concordant age of detrital zircons and the metamorphic age.

The timing of peak metamorphism of Ihosy has been inferred in various works by different researchers in the range of ca. 600–500 Ma (Andriamarofahatra et al., 1990; Paquette et al., 1994; Kröner et al., 1996; Nicollet et al., 1997; Markl et al., 2000; Jöns and Schenk, 2011; Collins et al., 2012). The timing of high-grade metamorphism and anatexis on rocks from Ihosy was documented by zircon ages between 526 ± 34 Ma and 557 ± 2 Ma with a mean age of about 550 Ma (Andriamarofahatra et al., 1990; Kröner et al., 1996). These ages were very similar to those obtained in Ihosy by Paquette et al. (1994) that interpreted the zircon ages between 580 Ma and 560 Ma to reflect the peak of high-grade metamorphism. Applying the electron microprobe monazite dating method for the Th–U–Pb system, Nicollet et al. (1997) inferred that the high-temperature metamorphism in Ihosy from southern Madagascar occurred at 560–550 Ma. Markl et al. (2000) suggested that the region experienced an earlier high-pressure and high-temperature event between 550 Ma and 530 Ma, and the metamorphic event was overprinted by lower-pressure metamorphism. Jöns and Schenk (2011) examined the petrology of meta-pelitic rock samples from the south area of the

Ranotsara shear zone near Ihosy and performed U–Pb SHRIMP dating on zircon and U-Th-Pb dating on monazite. In the whole Androyen group, Jöns and Schenk (2011) dated monazite at 560–530 Ma, and inferred UHT metamorphic event between 650 Ma and 600 Ma. Collins et al. (2012) dated foliated quartz + feldspar + biotite + sillimanite + cordierite gneiss from the Androyen Series at Ihosy and obtained metamorphic age of 531 ± 7 Ma from 10 analyses of zircons. In this study, sample MGK2-5I from Ihosy provided the timing of peak metamorphism as 514 ± 33 Ma by using the lower intercept age.

8.3. Comparison with *P–T* conditions and metamorphic ages in southern India

The result of the present study shows remarkable similarities to those from other continental fragments of Gondwana today dispersed around the Indian Ocean. The southern Madagascar is located at the central domain of the Gondwana supercontinent, with the southern part of India and further on with Sri Lanka and East Antarctica (Collins et al., 2014). This correlation was mainly based on structural arguments and the most important correlation marks are the shear zones found in southern Madagascar and southern India, here especially the Achankovil Suture Zone, which was interpreted to represent the continuation of the Ranotsara Shear Zone in Madagascar (Drury et al., 1984; Paquette et al., 1994; Windley et al., 1994; Kriegsman, 1995; Shackleton, 1996; Windley and Razakamanana, 1996; Rajesh et al., 1998; Martelat et al., 1999; Markl et al., 2000; Rajesh and Chetty, 2006).

Cordierite-bearing high-grade metasedimentary rocks are exposed along several localities in the Achankovil Suture Zone and have been the focus of several studies (Santosh, 1986; Nandakumar and Harley, 2000; Cenki et al., 2002; Ishii et al., 2006; Santosh et al., 2009; Shimizu et al., 2009; Johnson et al., 2015). Santosh (1986) first reported peak *P–T* conditions of 5.4–7.0 kbar and 710–790 °C for cordierite-bearing gneisses based on Fe–Mg exchange geothermobarometers of garnet-biotite, garnet-orthopyroxene and garnet-cordierite pairs. Nandakumar and Harley (2000) obtained *P–T* estimates of 6.5–7.5 kbar and 860–920 °C for cordierite gneisses from garnet-orthopyroxene geothermobarometer. Cenki et al. (2002) presented *P–T* calculations of 6–7 kbar and 900–950 °C for cordierite gneisses based on semi-quantitative pseudosection under KFMASH system and geothermobarometer of garnet-orthopyroxene and Al in orthopyroxene. Ishii et al. (2006) estimated peak metamorphic conditions at 8.5–9.5 kbar and 940–1040 °C for cordierite gneisses based on orthopyroxene bearing geothermobarometers and ternary feldspar geothermometer, suggesting UHT metamorphism. Shimizu et al. (2009) reported the results of geothermobarometric calculation of garnet-orthopyroxene assemblages in garnet-orthopyroxene-cordierite granulites that provides robust evidence for peak UHT metamorphism at 920–980 °C and 8–10 kbar, which was further confirmed by Al-in-Opx and magnetite–ilmenite geothermometers (900–950 °C and 1000 °C, respectively). Johnson et al. (2015) suggested a clockwise pressure–temperature path with peak metamorphic temperatures of up to 950 °C at pressures of around 0.7 GPa followed by high-temperature decompression for garnet-orthopyroxene gneiss. Tang et al. (2018) studied cordierite granulites from Kottayam and Munar in the Madurai Block at the north of the Achankovil Suture Zone, and obtained UHT conditions of 7.1–9.1 kbar/955–985 °C and clockwise *P–T* paths. Fig. 8 compares the similar clockwise *P–T* paths for cordierite gneisses from southern India (e.g. Ishii et al., 2006; Shimizu et al., 2009) and southern Madagascar. The detrital zircon ages from the study area (Fig. 9a and b; Kröner et al., 1996; Collins et al., 2012; this study) are also comparable with those from the cordierite gneiss from the Achankovil Suture Zone (Fig. 9c).

Analyses on homogeneous bright zircon rims generally suggest the age of high-grade metamorphism. Many previous studies interpreted the 550–500 Ma ages obtained from southern Madagascar and other Gondwana fragments to represent the peak metamorphic ages during the assembly of Gondwana supercontinent (e.g. Santosh et al., 2006; Collins et al., 2007; Sato et al., 2011; Johnson et al., 2015; Tang et al., 2018). In the Ranotsara shear zone, Collins et al. (2012) obtained metamorphic age of 531 ± 7 Ma from an Androyen Series sample near Ihosy. Kröner et al. (1996) documented zircon U-Pb ages between 526 ± 34 Ma and 557 ± 2 Ma to represent the timing of high-grade metamorphism and anatexis at Ihosy. In southern India, Collins et al. (2007) identified ca. 513 ± 6 Ma age that is interpreted as the timing of high-grade metamorphism throughout much of the Southern Granulite Terrane. Santosh et al. (2009) proposed that the 550–500 Ma age peaks commonly defined in previous studies might represent the post-peak thermal events, and the UHT metamorphism probably occurred at ca. 600–580 Ma. Clark et al. (2015) suggested that the UHT metamorphic conditions recorded in two metasedimentary gneisses from the Madurai Block were achieved at ca. 560 Ma. Furthermore, the zircon records share same distribution from Paleoproterozoic to Early Neoproterozoic detrital provenance and 550–500 Ma metamorphic ages (Fig. 9). Similar zircon ages and *P–T* paths have been obtained for cordierite gneisses from the Achankovil Suture Zone in southern India, which further confirm the Ranotsara Shear Zone is a continuation of the Achankovil Suture Zone (Fig. 10).

In addition to the similar rock types, detrital records, metamorphic condition and ages between the Ranotsara Shear Zone and the Achankovil Suture Zone, the lithological units at the both sides of the two zones also share comparable features. The Antananarivo Block at the north of the Ranotsara Shear Zone consists of 2550–2500 Ma felsic orthogneisses that are tectonically interlayered with voluminous 824–719 Ma granites, syenites and gabbros (Tucker et al., 1999; Kröner et al., 2000). The lithologies of the Antananarivo Block are comparable with the voluminous Neoarchean charnockite massifs (e.g., Collins et al., 2014) and Early to Middle Neoproterozoic gabbro–anorthosite complex (e.g. Kadavur region; Teale et al., 2011) in the northern part of the Madurai Block at the north of the Achankovil Suture Zone. Recently Neoproterozoic (938–632 Ma) arc magmatic rocks, which were subsequently metamorphosed at 567–510 Ma, have been reported from the southern part of the Madurai Block immediately north of the Achankovil Suture Zone (Santosh et al., 2017). Such Neoproterozoic ages from India are comparable with 1035–803 Ma magmatic ages for orthogneisses collected from east and northeast from our study area near Ihosy (Tucker et al., 2011). At the south of the Ranotsara Shear Zone, several north-south trending tectonic belts are composed of granulite- and high amphibolite-facies paragneiss, granulite and granite (e.g., Windley et al., 1994). As part of the Neoproterozoic metasedimentary belts, the Androyen Domain and Vohibory Domain is characterized by pelitic gneiss, marble, amphibolite and granitoid (Collins, 2006). Accordingly, the south of the Achankovil Suture Zone is represented by the Trivandrum Block which is dominated by metasedimentary gneisses that include garnet-bearing felsic gneisses and garnet + cordierite + sillimanite gneisses (khondalites) (Santosh et al., 2006; Collins et al., 2014). Thus, the Ranotsara Shear Zone in Madagascar connects the Achankovil Suture Zone in southern India, forming a major suture for the reconstruction of the Gondwanan supercontinent (Jöns and Schenk, 2011; Collins et al., 2014; Martelat et al., 2014).

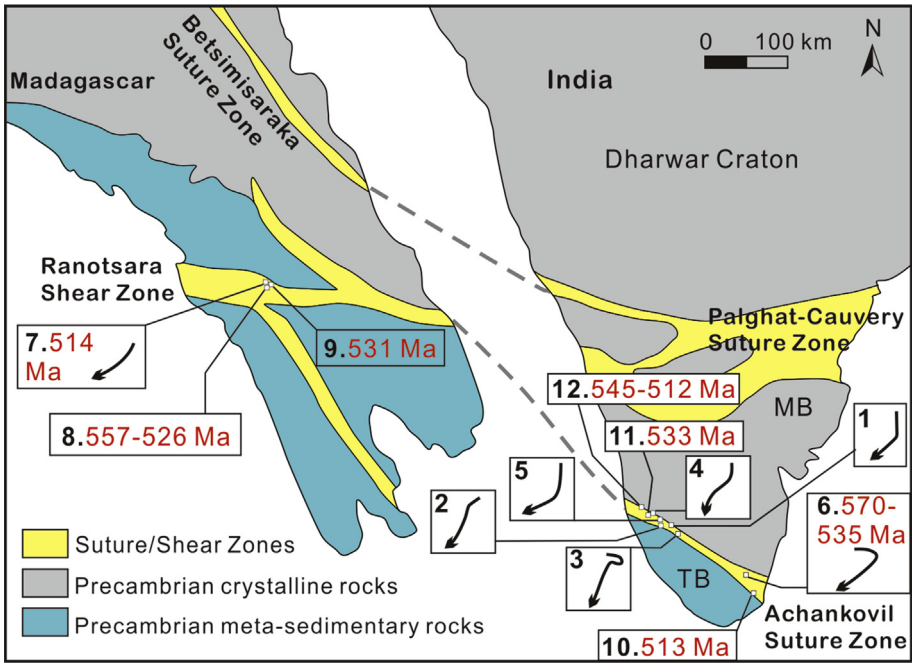

Figure 10. Simplified geological map of the southern India and Madagascar, showing the correlations, major basement rocks and suture/shear zones. *P–T* paths and peak metamorphic ages are sourced from 1: Santosh, 1987; 2: Nandakumar and Harley, 2000; 3: Cenki et al., 2002; 4: Ishii et al., 2006; 5: Shimizu et al., 2009; 6: Johnson et al., 2015; 7: this study; 8: Kröner et al., 1996; 9: Collins et al., 2012; 10: Collins et al., 2007; 11: Sato et al., 2010; 12: Collins et al., 2007; Tayler et al., 2015.

9. Conclusion

(1) Garnet-cordierite gneiss from Ihosy experienced two metamorphic stages of evolution. The mineral assemblages of garnet + sillimanite + cordierite (Crd-1) + quartz + plagioclase + K-feldspar + magnetite + spinel + ilmenite are stable during the peak metamorphism. The event was followed by a retrograde metamorphic stage represented by the mineral assemblage of biotite + garnet + cordierite (Crd-3) + quartz + plagioclase + K-feldspar + magnetite + spinel + ilmenite.

(2) Peak metamorphic *P–T* conditions of the garnet-cordierite gneiss are 850–960 °C and 6.9–7.7 kbar. The results define a clockwise *P–T* path, which involves peak UHT metamorphism and decompressional cooling during the retrograde stage with metamorphic *P–T* conditions of <740 °C and <4.8 kbar.

(3) Cores of detrital zircons in the garnet-cordierite gneiss indicate a wide age variation from the Middle to Late Paleoproterozoic (2030 Ma to 1784 Ma). The lower intercept age of 514 ± 33 Ma might imply the timing of high-grade metamorphism. The depositional age of the sediments, which were sourced from Paleoproterozoic rocks, is thus constrained at 1784–514 Ma.

(4) The petrological and geochronological data discussed in this study confirm that the Ranotsara Shear Zone in southern Madagascar could be a continuation of the Achankovil Suture Zone in southern India. They probably formed the same suture zone during the assembly of the Gondwana supercontinent.

Acknowledgements

We thank Geology Department of University of Antananarivo, Prof. Roger A. Rambeloson, Dr. E. Shaji, and Prof. M. Arima for valuable support of our fieldwork. We thank Dr. Tim Johnson and an anonymous reviewer for their constructive review comments, and Guest Editor Prof. Alan S. Collins for his editorial comments and suggestions. This work forms part of the MSc research of Meng Pan at the Graduate School of Life and Environmental Sciences, the University of Tsukuba. Partial funding for this project was produced by a Grant-in-Aid for Scientific Research (B) from Japan Society for the Promotion of Science (JSPS) to Tsunogae (Nos. 22403017, 26302009 and 18H01300).

Appendix A. Supplementary data

Supplementary data related to this article can be found at https://doi.org/10.1016/j.gsf.2018.05.014.

References

Ackermand, D., Windley, B.F., Razafiniparany, A., 1989. The Precambrian mobile belt of southern Madagascar. Geological Society London 43, 293–296. Special Publications.

Ackermand, D., Windley, B.F., Razafiniparany, A.H., 1991. Kornerupine breakdown reactions in paragneisses from southern Madagascar. Mineralogical Magazine 55, 71–80.

Agrawal, P.K., Pandey, O.P., Negi, J.G., 1992. Madagascar: a continental fragment of the paleo-super Dharwar craton of India. Geology 20, 543–546.

Almond, E.A., Timbres, D.H., Embury, J.D., 2013. The Influence of Second Phase Particles on Brittle Fracture, ICF2, Brighton (UK) 1969.

Andriamarofahatra, J., Delaboisse, H., Nicollet, C., 1990. Monazites and zircons U-Pb dating of the last major granulitic tectonometamorphic event in the south-eastern part of Madagascar. Comptes rendus de l academie des sciences serie ii 310, 1643–1648.

Boger, S.D., White, R.W., Schulte, B., 2012. The importance of iron speciation (Fe^{2+}/Fe^{3+}) in determining mineral assemblages: an example from the high-grade aluminous metapelites of southeastern Madagascar. Journal of Metamorphic Geology 30, 997–1018.

Boger, S.D., Hirdes, W., Ferreira, C.A.M., Jenett, T., Dallwig, R., Fanning, C.M., 2015. The 580–520 Ma Gondwana suture of Madagascar and its continuation into Antarctica and Africa. Gondwana Research 28, 1048–1060.

Bucher, K., Frey, M., 1994. Petrogenesis of Metamorphic Rocks. Springer-Verlag Berlin Heidelberg, p. 318.

Cenki, B., Kriegsman, L.M., Braun, I., 2002. Melt-producing and melt-consuming reactions in the Achankovil cordierite gneisses, South India. Journal of Metamorphic Geology 20, 543–561.

Chetty, T.R.K., Vijay, P., Narayana, B.L., Giridhar, G.V., 2003. Structure of the Nagavali shear zone, eastern Ghats mobile belt, India: correlation in the east Gondwana reconstruction. Gondwana Research 6, 215–229.

Clark, C., Healy, D., Johnson, T., Collins, A.S., Taylor, R.J., Santosh, M., Timms, N.E., 2015. Hot orogens and supercontinent amalgamation: a Gondwanan example from southern India. Gondwana Research 28, 1310–1328.
Collins, A.S., 2006. Madagascar and the amalgamation of central Gondwana. Gondwana Research 9, 3–16.
Collins, A.S., Windley, B.F., 2002. The tectonic evolution of central and northern Madagascar and its place in the final assembly of Gondwana. The Journal of Geology 110, 325–339.
Collins, A.S., Pisarevsky, S.A., 2005. Amalgamating eastern Gondwana: the evolution of the circum-Indian orogens. Earth Science Reviews 71, 229–270.
Collins, A.S., Santosh, M., Braun, I., Clark, C., 2007. Age and sedimentary provenance of the Southern Granulites, South India: U-Th-Pb SHRIMP secondary ion mass spectrometry. Precambrian Research 155, 125–138.
Collins, A.S., Kinny, P.D., Razakamanana, T., 2012. Depositional age, provenance and metamorphic age of metasedimentary rocks from southern Madagascar. Gondwana Research 21, 353–361.
Collins, A.S., Clark, C., Plavsa, D., 2014. Peninsular India in Gondwana: the tectonothermal evolution of the southern granulite terrain and its Gondwanan counterparts. Gondwana Research 25, 190–203.
Cox, R., Armstrong, R.A., Ashwal, L.D., 1998. Sedimentology, geochronology and provenance of the Proterozoic Itremo Group, central Madagascar, and implications for pre-Gondwana palaeogeography. Journal of the Geological Society 155, 1009–1024.
de Wit, M.J., Vitali, E., Ashwal, L., 1995. Gondwana reconstruction of the east Africa-Madagascar-India-Sri Lanka-Antarctica fragments revised. Centennial Geocongress Extended Abstracts 1, 218–221.
de Wit, M.J., Bowring, S.A., Ashwal, L.D., Randrianasolo, L.G., Morel, V.P.I., Rambeloson, R.A., 2001. Age and tectonic evolution of Neoproterozoic ductile shear zones in southwestern Madagascar, with implications for Gondwana studies. Tectonics 20, 1–45.
Drury, S.A., Harris, N.B.W., Holt, R.W., Reeves-Smith, G.J., Wightman, R.T., 1984. Precambrian tectonics and crustal evolution in South India. The Journal of Geology 92, 3–20.
Endo, T., Tsunogae, T., Santosh, M., Shaji, E., Rambeloson, R.A., 2017. Petrogenesis of incipient charnockite in the Ikalamavony sub-domain, south-central Madagascar: new insights from phase equilibrium modeling. Lithos 282–283, 431–446.
Fitzsimons, I.C.W., Hulscher, B., 2005. Out of Africa: detrital zircon provenance of central Madagascar and Neoproterozoic terrane transfer across the Mozambique Ocean. Terra Nova 17, 224–235.
Fitzsimons, I.C., 2016. Pan–African granulites of Madagascar and southern India: Gondwana assembly and parallels with modern Tibet. Journal of Mineralogical and Petrological Sciences 111, 73–88.
Ghosh, J.G., de Wit, M.J., Zartman, R.E., 2004. Age and tectonic evolution of Neoproterozoic ductile shear zones in the Southern Granulite Terrain of India, with implications for Gondwana studies. Tectonics, 2002TC001444.
Grégoire, V., Nédélec, A., 1997. Pan-African Andringitean granites of Madagascar: structure and P–T emplacement conditions. Terra Nova 9 Abstract Supplement 1, 464.
Harley, S.L., 1989. The origin of granulites: a metamorphic perspective. Geological Magazine 126, 215–247.
Harris, N., 1999. The significance of the Palghat-Cauvery shear zone in southern India for correlations between south-west India and eastern Madagascar. Gondwana Research 2, 471–472.
He, X.-F., Santosh, M., Tsunogae, T., Malaviarachchi, S.P.K., 2016a. Early to late Neoproterozoic magmatism and magma mixing - mingling in Sri Lanka: implications for convergent margin processes during Gondwana assembly. Gondwana Research 32, 151–180.
He, X.-F., Santosh, M., Tsunogae, T., Malaviarachchi, S.P.K., Dharmapriya, P.L., 2016b. Neoproterozoic arc accretion along the 'eastern suture' in Sri Lanka during Gondwana assembly. Precambrian Research 279, 57–80.
Hiroi, Y., Ogo, Y., Namba, K., 1994. Evidence for prograde metamorphic evolution of Sri Lankan pelitic granulites, and implications for the development of continental crust. Precambrian Research 66, 245–263.
Holland, T.J.B., Powell, R., 1998. An internally consistent thermodynamic data set for phases of petrological interest. Journal of Metamorphic Geology 16, 309–343.
Holland, T.J.B., Powell, R., 2003. Activity–composition relations for phases in petrological calculations: an asymmetric multicomponent formulation. Contributions to Mineralogy and Petrology 145, 492–501.
Horie, K., Takehara, M., Suda, Y., Hidaka, H., 2013. Potential Mesozoic reference zircon from the Unazuki plutonic complex: geochronological and geochemical characterization. Island Arc 22, 292–305.
Ishii, S., Tsunogae, T., Santosh, M., 2006. Ultrahigh-temperature metamorphism in the Achankovil Zone: implications for the correlation of crustal blocks in southern India. Gondwana Research 10, 99–114.
Jacobs, J., Falter, M., Thomas, R.J., Kunz, J., Jeßberger, E.K., 1997. $^{40}Ar/^{39}Ar$ thermochronological constraints on the structural evolution of the mesoproterozoic natal metamorphic Province, SE Africa. Precambrian Research 86, 71–92.
Jacobs, J., Fanning, C.M., Henjes-Kunst, F., Olesch, M., Paech, H.J., 1998. Continuation of the Mozambique belt into east Antarctica: grenville-age metamorphism and polyphase Pan-African high-grade events in central Dronning Maud Land. The Journal of Geology 106, 385–406.
Janardhan, A.S., Anto, F., Sivasubramanian, P., 1997. Granulite blocks of southern India: implications for South India–Madagascar reconstruction. Gondwana Research Group Miscellaneous Publication 5, 33.
Janardhan, A.S., 1999. Southern granulite terrain, south of the Palghat-Cauvery shear zone: implications for India-Madagascar connection. Gondwana Research 2, 463–469.
Johnson, T.E., Clark, C., Taylor, R.J.M., Santosh, M., Collins, A.S., 2015. Prograde and retrograde growth of monazite in migmatites: an example from the Nagercoil Block, southern India. Geoscience Frontiers 6, 373–387.
Jöns, N., Schenk, V., 2011. The ultrahigh temperature granulites of southern Madagascar in a polymetamorphic context: implications for the amalgamation of the Gondwana supercontinent. European Journal of Mineralogy 23, 127–156.
Katz, M.B., Premoli, C., 1979. India and Madagascar in Gondwanaland based on matching Precambrian lineaments. Nature 279, 312–315.
Kennedy, W.Q., 1964. The structural differentiation of Africa in the Pan-African (±500 My) tectonic episode. Research Institute of African Geology University of Leeds Annual Report 8, 48–49.
Kretz, R., 1983. Symbols for rock-forming minerals. American Mineralogist 68, 277–279.
Kriegsman, L.M., 1995. The Pan-African event in East Antarctica: a view from Sri Lanka and the Mozambique belt. Precambrian Research 75, 263–277.
Kröner, A., 1984. Late Precambrian plate tectonics and orogeny: a need to redefine the term Pan-African. In: Klerkx, J., Michot, J. (Eds.), African Geology. Tervuren Museé R. l'Afrique Centrale, Belgium, pp. 23–28.
Kröner, A., Braun, I., Jaeckel, P., 1996. Zircon geochronology of anatectic melts and residues from a high-grade pelitic assemblage at Ihosy, southern Madagascar: evidence for Pan-African granulite metamorphism. Geological Magazine 133, 311–323.
Kröner, A., Windley, B.F., Jaeckel, P., Brewer, T.S., Razakamanana, T., 1999. New zircon ages and regional significance for the evolution of the Pan-African orogen in Madagascar. Journal of the Geological Society London 156, 1125–1135.
Kröner, A., Hegner, H., Collins, A.S., Windley, B.F., Brewer, T.S., Razakamanana, T., Pidgeon, R.T., 2000. Age and magmatic history of the Antananarivo Block, central Madagascar, as derived from zircon geochronology and Nd isotopic systematics. American Journal of Science 300, 251–288.
Kröner, A., Kehelpannala, K.V.W., Hegner, E., 2003. Ca. 750–1100 Ma magmatic events and Grenville-age deformation in Sri Lanka: relevance for Rodinia supercontinent formation and dispersal, and Gondwana amalgamation. Journal of Asian Earth Sciences 22, 279–300.
Kröner, A., Santosh, M., Wong, J., 2012. Zircon ages and Hf isotopic systematics reveal vestiges of Mesoproterozoic to Archaean crust within the late Neoproterozoic–Cambrian high-grade terrain of southernmost India. Gondwana Research 21, 876–886.
Korhonen, F.J., Brown, M., Clark, C., Bhattacharya, S., 2013. Osumilite–melt interactions in ultrahigh temperature granulites: phase equilibria modelling and implications for the P–T–t evolution of the Eastern Ghats Province, India. Journal of Metamorphic Geology 31, 881–907.
Leake, B.E., Woolley, A.R., Arps, C.E.S., Birch, W.D., Gilbert, M.C., Grice, J.D., Hawthorne, F.C., Kato, A., Kisch, H.J., Krivovichev, V.G., Linthout, K., Laird, J., Mandarino, J.A., Maresch, W.V., Nickel, E.H., Rock, N.M.S., Schumacher, J.C., Smith, D.C., Stephenson, N.C.N., Ungaretti, L., Whittaker, E.J.W., Youzhi, G., 1997. Nomenclature of amphiboles: report of the subcommittee on amphiboles of the International Mineralogical Association, commission on new minerals and mineral names. American Mineralogist 82, 1019–1037.
Li, S.S., Santosh, M., Indu, G., Shaji, E., Tsunogae, T., 2017. Detrital zircon geochronology of quartzites from the southern Madurai Block, India: implications for Gondwana reconstruction. Geoscience Frontiers 8, 851–867.
Ludwig, K.R., 2003. ISOPLOT 3.00: a Geochronological Toolkit for Microsoft Excel. Berkeley Geochronology Center, California, Berkeley, p. 39.
Markl, G., Bäuerle, J., Grujic, D., 2000. Metamorphic evolution of Pan-African granulite facies metapelites from southern Madagascar. Precambrian Research 102, 47–68.
Martelat, J.E., Nicollet, C., Lardeaux, J.M., Vidal, G., Rakotondrazafy, R., 1997. Lithospheric tectonic structures developed under high-grade metamorphism in the southern part of Madagascar. Geodinamica Acta 10, 94–114.
Martelat, J.E., Schulmann, K., Lardeaux, J.M., Nicollet, C., Cardon, H., 1999. Granulite microfabrics and deformation mechanisms in southern Madagascar. Journal of Structural Geology 21, 671–687.
Martelat, J.E., Malamoud, K., Cordier, P., Randrianasolo, B., Schulmann, K., Lardeaux, J.M., 2012. Garnet crystal plasticity in the continental crust, new example from south Madagascar. Journal of Metamorphic Geology 30, 435–452.
Martelat, J.E., Randrianasolo, B., Schulmann, K., Lardeaux, J.M., Devidal, J.L., 2014. Airborne magnetic data compared to petrology of crustal scale shear zones from southern Madagascar: a tool for deciphering magma and fluid transfer in orogenic crust. Journal of African Earth Sciences 94, 74–85.
Mosley, P.N., 1993. Geological evolution of the late proterozoic "Mozambique belt" of Kenya. Tectonophysics 221, 223–250.
Nandakumar, V., Harley, S.L., 2000. A reappraisal of the pressure-temperature path of granulites from the Kerala Khondalite Belt, southern India. The Journal of Geology 108, 687–703.
Nédélec, A., Ralison, B., Bouchez, J.L., Grégoire, V., 2000. Structure and metamorphism of the granitic basement around Antananarivo: a key to the Pan-African history of central Madagascar and its Gondwana connections. Tectonics 19, 997–1020.
Nicollet, C., 1985. The banded cordierite and garnet-bearing gneisses from Ihosy – a geothermo-barometric tracer in southern Madagascar. Precambrian Research 28, 175–185.
Nicollet, C., 1990. Crustal evolution of the granulites of Madagascar. In: Vielzeuf, D., Vidal, Ph (Eds.), Granulites and Crustal Evolution. NATO ASI Series 311. Springer, pp. 291–310.

Nicollet, C., Montel, J.M., Foret, S., Martelat, J.E., Rakotondrazafy, R., Lardeaux, J.M., 1997. E-Probe monazite dating in Madagascar: a good example of the usefulness of the in-situ dating method. UNESCO IUGS IGCP 348, 65.
Paces, J.B., Miller, J.D., 1993. Precise U–Pb ages of Duluth Complex and related mafic intrusions, northeastern Minnesota: geochronological insights to physical, petrogenetic, paleomagnetic and tectonomagmatic processes associated with the 1.1 Ga midcontinent rift system. Journal of Geophysical Research 98, 13997–14013.
Paquette, J.L., Nédélec, A., Moine, B., Rakotondrazafy, M., 1994. U-Pb, single zircon Pb-evaporation, and Sm-Nd isotopic study of a granulite domain in SE Madagascar. The Journal of Geology 102, 523–538.
Piazolo, S., Markl, G., 1999. Humite-and scapolite-bearing assemblages in marbles and calcsilicates of Dronning Maud Land, Antarctica: new data for Gondwana reconstructions. Journal of Metamorphic Geology 17, 91–107.
Pili, E., Ricard, Y., Lardeaux, J.M., Sheppard, S.M.F., 1997. Lithospheric shear zones and mantle-crust connections. Tectonophysics 280, 15–29.
Plavsa, D., Collins, A.S., Foden, J.F., Kropinski, L., Santosh, M., Chetty, T.R.K., Clark, C., 2012. Delineating crustal domains in Peninsular India: age and chemistry of orthopyroxene-bearing felsic gneisses in the Madurai Block. Precambrian Research 198, 77–93.
Plavsa, D., Collins, A.S., Foden, J.D., Clark, C., 2015. The evolution of a Gondwanan collisional orogen: a structural and geochronological appraisal from the Southern Granulite Terrane, South India. Tectonics 34, 820–857.
Raith, M.M., Rakotondrazafy, R., Sengupta, P., 2008. Petrology of corundum-spinel-sapphirine-anorthite rocks (sakenites) from the type locality in southern Madagascar. Journal of Metamorphic Geology 26, 647–667.
Rajesh, H.M., Santosh, M., Yoshida, M., 1998. Dextral Pan-African shear along the southwestern edge of the Achankovil Shear Belt, south India: constraints on Gondwana reconstructions: a discussion. The Journal of Geology 106, 105–114.
Rajesh, K.G., Chetty, T.R.K., 2006. Structure and tectonics of the Achankovil shear zone, southern India. Gondwana Research 10, 86–98.
Rakotonandrasana, N.O.T., Arima, M., Miyawaki, R., Rambeloson, R.A., 2010. Widespread occurrences of högbomite-2N2S in UHT metapelites from the Betroka Belt, Southern Madagascar: implications on melt or fluid activity during regional metamorphism. Journal of Petrology 51, 869–895.
Rambeloson, A.R., 1999. Gold in Madagascar. Gondwana Research 2, 423–431.
Rindraharisaona, E.J., Tilmann, F., Yuan, X., Rümpker, G., Giese, J., Rambolamanana, G., Barruol, G., 2017. Crustal structure of southern Madagascar from receiver functions and ambient noise correlation: implications for crustal evolution. Journal of Geophysical Research Solid Earth 122, 1179–1197.
Santosh, M., 1986. Carbonic metamorphism of charnockites in the southwestern Indian Shield: a fluid inclusion study. Lithos 19, 1–10.
Santosh, M., 1987. Cordierite gneisses of southern Kerala, India: petrology, fluid inclusions and implications for crustal uplift history. Contributions to Mineralogy and Petrology 96, 343–356.
Santosh, M., Tanaka, K., Yokoyama, K., Collins, A.S., 2005. Late Neoproterozoic-Cambrian felsic magmatism along transcrustal shear zones in southern India: U-Pb electron microprobe ages and implications for the amalgamation of the Gondwana supercontinent. Gondwana Research 8, 31–42.
Santosh, M., Morimoto, T., Tsutsumi, Y., 2006. Geochronology of the khondalite belt of Trivandrum Block, southern India: electron probe ages and implications for Gondwana tectonics. Gondwana Research 9, 261–278.
Santosh, M., Maruyama, S., Sato, K., 2009. Anatomy of a Cambrian suture in Gondwana: Pacific-type orogeny in southern India? Gondwana Research 16, 321–341.
Santosh, M., Tsunogae, T., Malaviarachchi, S.P.K., Zhang, Z., Ding, H., Tang, L., Dharmapriya, P.L., 2014. Neoproterozoic crustal evolution in Sri Lanka: insights from petrologic, geochemical and zircon U-Pb and Lu-Hf isotopic data and implications for Gondwana assembly. Precambrian Research 255, 1–29.
Santosh, M., Yang, Qiong-Yan, Shaji, E., Tsunogae, T., Ram Mohan, M., Satyanarayanan, M., 2015. An exotic Mesoarchean microcontinent: the Coorg Block, southern India. Gondwana Research 27, 165–195.
Santosh, M., Yang, Q.Y., Shaji, E., Ram Mohan, M., Tsunogae, T., Satyanarayanan, M., 2016. Oldest rocks from Peninsular India: evidence for Hadean to neoarchean crustal evolution. Gondwana Research 29, 105–135.
Santosh, M., Hu, C.N., He, X.F., Li, S.S., Tsunogae, T., Shaji, E., Indu, G., 2017. Neoproterozoic arc magmatism in the southern Madurai block, India: subduction, relamination, continental outbuilding, and the growth of Gondwana. Gondwana Research 45, 1–42.
Sato, K., Santosh, M., Tsunogae, T., Kon, Y., Yamamoto, S., Hirata, T., 2010. Laser ablation ICP mass spectrometry for zirconU-Pb geochronology of ultrahigh-temperature gneisses and A-type granites from the Achankovil Suture Zone, southern India. Journal of Geodynamics 50, 286–299.
Sato, K., Santosh, M., Tsunogae, T., Chetty, T.R.K., Hirata, T., 2011. Subduction–accretion–collision history along the Gondwana suture in southern India: a laser ablation ICP-MS study of zircon chronology. Journal of Asian Earth Sciences 40, 162–171.
Schreurs, G., Giese, J., Berger, A., Gnos, E., 2006. The role of the Ranotsara Zone in southern Madagascar for Gondwana correlations. In: 11. Symposium" Tektonik, Struktur-und Kristallingeologie. Universitätsverlag Göttingen, pp. 198–201.
Schumacher, R., Schenk, V., Raase, P., Vitanage, P.W., 1990. Granulite facies metamorphism of metabasic and intermediate rocks in the Highland Series of Sri Lanka. In: High-temperature Metamorphism and Crustal Anatexis. Springer, pp. 235–271.
Shackleton, R.M., 1996. The final collision zone between East and West Gondwana: where is it? Journal of African Earth Sciences 23, 271–287.
Shimizu, H., Tsunogae, T., 2010. Field occurrence of cordierite gneiss and related ultrahigh-temperature granulites from the Achankovil Shear Zone, southern India. Earth Evolution Sciences 4, 13–22.
Shimizu, H., Tsunogae, T., Santosh, M., 2009. Spinel + quartz assemblage in granulites from the Achankovil Shear Zone, southern India: implications for ultrahigh-temperature metamorphism. Journal of Asian Earth Sciences 36, 209–222.
Shiraishi, K., Ellis, D.J., Hiroi, Y., Fanning, C.M., Motoyoshi, Y., Nakai, Y., 1994. Cambrian orogenic belt in East Antarctica and Sri Lanka: implications for Gondwana assembly. The Journal of Geology 102, 47–65.
Stacey, J.T., Kramers, J., 1975. Approximation of terrestrial lead isotope evolution by a two-stage model. Earth and Planetary Science Letters 26, 207–221.
Strachan, R.A., Collins, A.S., Buchan, C., Nance, R.D., Murphy, J.B., D'Lemos, R.S., 2007. Terrane analysis along a Neoproterozoic active margin of Gondwana: insights from U–Pb zircon geochronology. Journal of the Geological Society 164, 57–60.
Takahashi, K., Tsunogae, T., Santosh, M., Takamura, Y., Tsutsumi, Y., 2018. Paleoproterozoic (ca. 1.8 Ga) arc magmatism in the Lützow-Holm Complex, East Antarctica: implications for crustal growth and terrane assembly in erstwhile Gondwana fragments. Journal of Asian Earth Sciences 157, 245–268.
Takamura, Y., Tsunogae, T., Santosh, M., Malaviarachchi, S.P.K., Tsutsumi, Y., 2015. Petrology and zircon U-Pb geochronology of metagabbro from the Highland Complex, Sri Lanka: implications for the correlation of Gondwana suture zones. Journal of Asian Earth Sciences 113, 826–841.
Takamura, Y., Tsunogae, T., Santosh, M., Tsutsumi, Y., 2018. Detrital zircon geochronology of the Lützow-Holm complex, east Antarctica: implications for Antarctica – Sri Lanka correlation. Geoscience Frontiers 9, 355–375.
Tang, L., Santosh, M., Tsunogae, T., Koizumi, T., Hu, X.K., Teng, X.M., 2017. Petrology, phase equilibria modelling and zircon U–Pb geochronology of Paleoproterozoic mafic granulites from the Fuping Complex, North China Craton. Journal of Metamorphic Geology 35, 517–540.
Tang, L., Rajesh, S., Santosh, M., Tsunogae, T., Pradeepkumar, A.P., Tsutsumi, Y., Takamura, Y., 2018. Metamorphic phase equilibria modelling and zircon U–Pb geochronology of ultrahigh-temperature cordierite granulites from the Madurai Block, India: implications for hot Gondwana crust. International Geology Review 60, 21–42.
Taylor, R.J.M., Clark, C., Johnson, T.E., Santosh, M., Collins, A.S., 2015. Unravelling the complexities in high-grade rocks using multiple techniques: the Achankovil Zone of southern India. Contributions to Mineralogy and Petrology 169, 1–19.
Teale, W., Collins, A.S., Foden, J., Payne, J.L., Plavsa, D., Chetty, T.R.K., Santosh, M., Fanning, M., 2011. Cryogenian (830 Ma) mafic magmatism and metamorphism in the northern Madurai Block, southern India: a magmatic link between Sri Lanka and Madagascar? Journal of Asian Earth Sciences 42, 223–233.
Tsunogae, T., Endo, T., Santosh, M., Thierry Rakotonandrasana, N.O., Shaji, E., Rambeloson, R.A., 2013. Phase Equilibrium Modeling of Pan-African Incipient Charnockite from Southern Madagascar, EGU General Assembly Conference Abstracts, p. 14087.
Tsunogae, T., Dunkley, D.J., Horie, K., Endo, T., Miyamoto, T., Kato, M., 2014. Petrology and SHRIMP zircon geochronology of granulites from Vesleknausen, Lützow-Holm Complex, East Antarctica: Neoarchean magmatism and Neoproterozoic high-grade metamorphism. Geoscience Frontiers 5, 167–182.
Tsunogae, T., Yang, Q.Y., Santosh, M., 2015. Early Neoproterozoic arc magmatism in the Lützow-Holm Complex, East Antarctica: petrology, geochemistry, zircon U–Pb geochronology and Lu–Hf isotopes and tectonic implications. Precambrian Research 266, 467–489.
Tsunogae, T., Yang, Q.Y., Santosh, M., 2016. Neoarchean–Early Paleoproterozoic and Early Neoproterozoic arc magmatism in the Lützow–Holm complex, East Antarctica: insights from petrology, geochemistry, zircon U–Pb geochronology and Lu–Hf isotopes. Lithos 263, 239–256.
Tsutsumi, Y., Horie, K., Sano, T., Miyawaki, R., Momma, K., Matsubara, S., Shigeoka, M., Yokoyama, K., 2012. LA-ICP-MS and SHRIMP ages of zircons in chevkinite and monazite tuffs from the Boso Peninsula, Central Japan. Bulletin of the National Museum of Nature and Science Series C 38, 15–32.
Tucker, R.D., Ashwal, L.D., Handke, M.J., Hamilton, M.A., Le Grange, M., Rambeloson, R.A., 1999. U-Pb geochronology and isotope geochemistry of the Archean and Proterozoic rocks of north-central Madagascar. The Journal of Geology 107, 135–153.
Tucker, R.D., Roig, J.Y., Macey, P.H., Delor, C., Amelin, Y., Armstrong, R.A., Rabarimanana, M., Ralison, A.V., 2011. A new geological framework for south-central Madagascar, and its relevance to the "out-of-Africa" hypothesis. Precambrian Research 185, 109–130.
White, R.W., Powell, R., Holland, T.J.B., Worley, B.A., 2000. The effect of TiO_2 and Fe_2O_3 on metapelitic assemblages at greenschist and amphibolite facies conditions: mineral equilibria calculations in the system K_2O-FeO-MgO-Al_2O_3-SiO_2-H_2O-TiO_2-Fe_2O_3. Journal of Metamorphic Geology 18, 497–511.
White, R.W., Powell, R., Clarke, G.L., 2002. The interpretation of reaction textures in Fe-rich metapelitic granulites of the Musgrave Block, central Australia: constraints from mineral equilibria calculations in the system K_2O-FeO-MgO-Al_2O_3-SiO_2-H_2O-TiO_2-Fe_2O_3. Journal of Metamorphic Geology 20, 41–55.
White, R.W., Powell, R., Holland, T.J.B., 2007. Progress relating to calculation of partial melting equilibria for metapelites. Journal of Metamorphic Geology 25, 511–527.
Windley, B.F., Razafiniparany, A., Razakamanana, T., Ackermand, D., 1994. Tectonic framework of the Precambrian of Madagascar and its Gondwana connections: a review and reappraisal. Geologische Rundschau 83, 642–659.
Windley, B.F., Razakamanana, T., 1996. The Madagascar-India connection in a Gondwana framework. The Archaean and proterozoic terranes in southern India within east Gondwana Gondwana research group. Memoir 3, 25–37.